07PFL-518

Unthrottled Engine Operation using Variable Valve Actuation: The Impact on the Flow Field, Mixing and Combustion

Philip A. Stansfield, Graham Wigley, Colin P. Garner
Faculty of Engineering, Loughborough University, Leicestershire, LE11 3TU, UK.

Rishin Patel, Nicos Ladommatos
Department of Mechanical Engineering, University College London, London, WC1E 7JE, UK

Graham Pitcher, Jamie W.G. Turner
Powertrain Research, Lotus Engineering Ltd, Hethel, Norwich, NR14 8EZ, UK

Hans Nuglisch, Jerome Helie
Siemens VDO Automotive S.A.S., 31036 Toulouse, France

ABSTRACT

The effect on the intake flow field, air fuel mixing processes, thermodynamic performance and emissions output has been investigated for a range of valve operating profiles. A standard speed load point of 2000 rpm and 2.7 bar $IMEP_{720°}$ has been reached by throttling the intake whilst running standard cam profiles, by early closing of both inlet valves (EIVC) and by early closing of each inlet individually to generate bulk swirl motions within the cylinder. Data has been recorded at stoichiometric air fuel ratios for both direct injection and port fuelled operation.

The valve profiles have been applied to two single cylinder homogeneous gasoline direct injection (GDI) spark ignition engines, developed to investigate the potential of controlling engine load by limiting the inducted air mass using fully variable valve timing (FVVT) to reduce pumping losses at part load. The first engine featured a full length optical liner, allowing 2D Particle Image Velocimetry (PIV) measurements of the intake flow fields to be made, along with Mie imaging studies of the liquid fuel fraction. The second was a thermodynamic engine equipped to measure specific fuel consumption and emissions of CO_2, CO, NO_X and THC.

The work shows that fuel economy benefits can be gained by operating the engine with unthrottled EIVC operation. However, the interaction between the intake air and direct injection fuel spray means performance is highly dependant upon which valve is operated and the timing of the direct injection fuel spray.

INTRODUCTION

Climate change is forcing many technologies to be investigated and developed with the aim of reducing man-made emissions of greenhouse gases (GHG). European automobile manufacturers (ACEA) have made a voluntary commitment to reduce average CO_2 emissions across the new car fleet to 140g CO_2 per km by the year 2008 [1]. It has also been suggested that an EU proposal of 120g CO_2 per km may be implemented by 2012 [1].

In an attempt to meet these emissions targets, several new technologies have been commercialised with many others being developed to differing states of readiness. One technology is Gasoline Direct Injection (GDI). GDI was originally developed for aeronautical applications [2], but remained dormant in automotive applications until being resurrected by Mitsubishi as a means of enabling stratified combustion in road-going engines [3]. The ability to run a stratified charge allowed engines to run with excess air in the cylinder, reducing the throttle required and hence reducing the associated pumping losses and therefore improving the thermodynamic efficiency. However, initial 'wall-guided' combustion systems could not realise the full benefit of GDI due to the challenges in controlling the fuel spray in the combustion chamber. As a consequence, the area of stratified operation was relatively small and, over a standard drive cycle, the fuel consumption benefit was only a few percent [4].

The fuel economy of these 'first generation' lean burn GDI systems was further eroded by the necessity to fit a NOx 'trap' in order to meet Euro 4 emissions requirements. Such traps are expensive and demand a frequent period of rich operation to regenerate, which incurs a fuel consumption penalty. They are also poisoned by the high sulphur content in gasoline fuel currently on sale in most of Europe and the United States [5].

Therefore, incremental development steps have been made towards the introduction of 'spray-guided' engines, where the stratified charge is generated by the fuel spray's proximity to the spark plug [4]. The spray guided arrangement allows the area of stratified operation to be extended and improves the overall fuel economy [1].

Both wall guided and spray guided systems aim to operate the engine with a wider-open throttle for any given part-load condition, thus allowing a reduction in the throttling losses. These losses can alternatively be addressed by the use of Fully Variable Valve Trains (FVVT) [6, 7].

FVVT's are currently being developed to production readiness [8,9]. These allow Early Inlet Valve Closing (EIVC) and Late Inlet Valve Closing (LIVC) strategies to be applied, together with many other possibilities such as skip-firing and rolling cylinder deactivation. Arguably, the most advanced systems are electro-hydraulic types with closed-loop control. Research systems have been available for sometime, but recent interest in homogenous charge compression ignition (HCCI) has accelerated interest in their use to develop cam profile switching and phasing mechanisms. Electro-hydraulic systems offer the highest degree of control and are applicable to both gasoline and Diesel engines. As the motion of each valve is followed and controlled individually in real time, electro-hydraulic systems offer superior piston collision avoidance.

FVVT and GDI technologies achieve the same goal, namely reduction of throttling losses at part load, however, other advantages can be realised by combining the technologies [10]. Start-up catalyst light-off can be accelerated through late intake valve opening (LIVO) strategies with reduced fuel consumption afforded by the lower requirement for cold-start fuelling from direct injection, and, since the in-cylinder air flow can be influenced by the valve motion, combustion can be accelerated under some part load conditions. Rolling cylinder deactivation without fuel collecting in the intake port is also a possibility in multi-cylinder engines, together with the opportunity to run cylinders at different loads or in different combustion modes. There are thus synergies between the technologies beyond throttling loss reduction.

Homogeneous charge operation of a DISI engine allows conventional after-treatment to be used in the form of a three-way catalyst and the requirement for a NOx trap and low sulphur gasoline are removed. This means a lower bill of material (BOM) cost for the vehicle exhaust system components and world-wide fuel compatibility.

The effect on the in-cylinder flow field of varying the intake valve profiles is known to significantly affect the air-fuel mixing and hence the combustion performance and emissions output. The variation of in-cylinder flow with valve profile has not been extensively studied. The aim of the current work is to investigate the air motion and air fuel mixing processes occurring within the cylinder and relate these physical processes to engine performance, emissions output and fuel economy.

RESEARCH ENGINES

Two research engines, one designed for optical studies and the other for analysing thermodynamic performance, were fitted with identical combustion chamber geometries (Bore: 88.0 mm, Stroke: 82.1 mm, Compression ratio: 10:1) and identical inlet and exhaust systems. Engine diagnostic equipment was duplicated on both engines.

Both engines were operated at a standard test point of 2000 rpm and 2.7 bar IMEP, where the IMEP was calculated over a 720° cycle to include pumping losses. This test point was achieved using three inlet valve strategies (Figure 1).

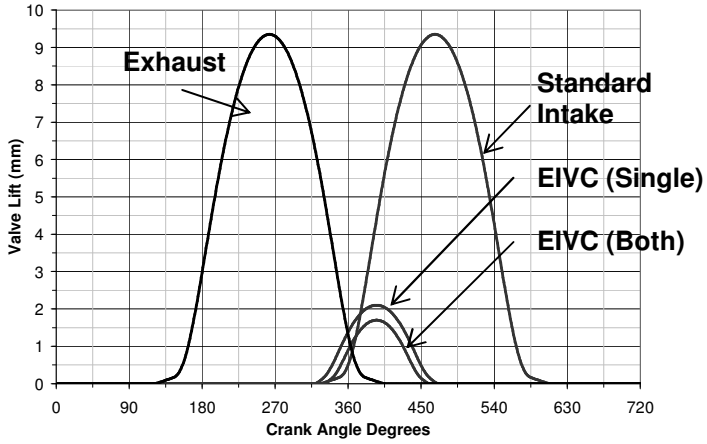

Figure 1: Valve profiles to achieve 2.7 bar $IMEP_{720°}$

Firstly, the engine was throttled whilst running 'standard' production valve profiles. Secondly, the lift and duration of the inlet cam was reduced for unthrottled EIVC. Finally, each inlet valve was opened independently, for single valve EIVC operation, to investigate the effect of opposite bulk swirl motions within the cylinder. The profiles required to achieve the test point were calculated on a 1D engine simulation code and verified using the

optical engine under firing conditions but fitted with a steel liner (Table 1).

Table 1: Valve profiles to achieve 2.7 bar $IMEP_{720°}$

Intake Std	IVO = 345º	IVC = 585º	Lift: 9.35 mm
EIVC (Both)	IVO = 335º	IVC = 451º	Lift: 1.70 mm
EIVC (Single)	IVO = 325º	IVC = 462º	Lift: 2.10 mm
Exhaust	EVO = 135º	EVC = 375º	Lift: 9.35 mm

The respective PV diagrams showing the potential for EIVC cycle pumping loss benefits are shown in Figure 2.

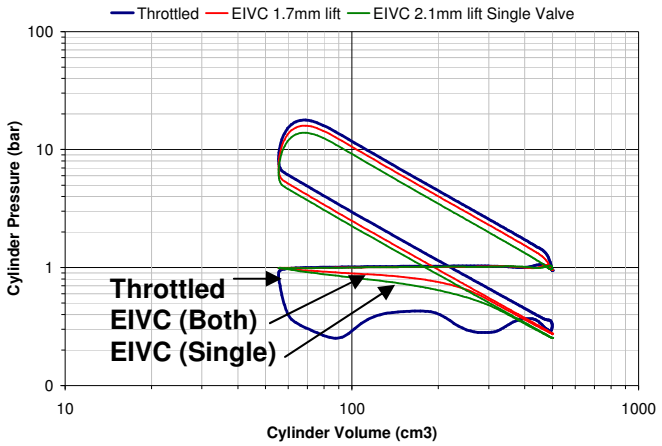

Figure 2: PV Diagrams for Valve Strategies 2000 rpm, 2.7 bar $IMEP_{720°}$

OPTICAL ENGINE

The Single Cylinder Optical Research Engine (SCORE), has been designed by Lotus Engineering specifically for the application of optical diagnostic techniques (Figure 3). The engine incorporates a full length fused silica liner and a sapphire window in the piston crown to provide extensive optical access to the combustion chamber. The piston contains a carbon fibre piston ring which runs in the optical liner to maintain compression pressures. It has both primary and secondary balance shafts to allow operation at speeds of up to 5000 rpm. Engine timing data is provided by two optical encoders, one with 0.2° resolution mounted on a 2:1 drive which represented the camshaft timing and provided the maximum resolution of the laser diagnostic system. The second encoder provided a TDC pulse from the crankshaft and a 1.0° resolution pulse for the Active Valve Train (AVT) timing system and engine diagnostic system.

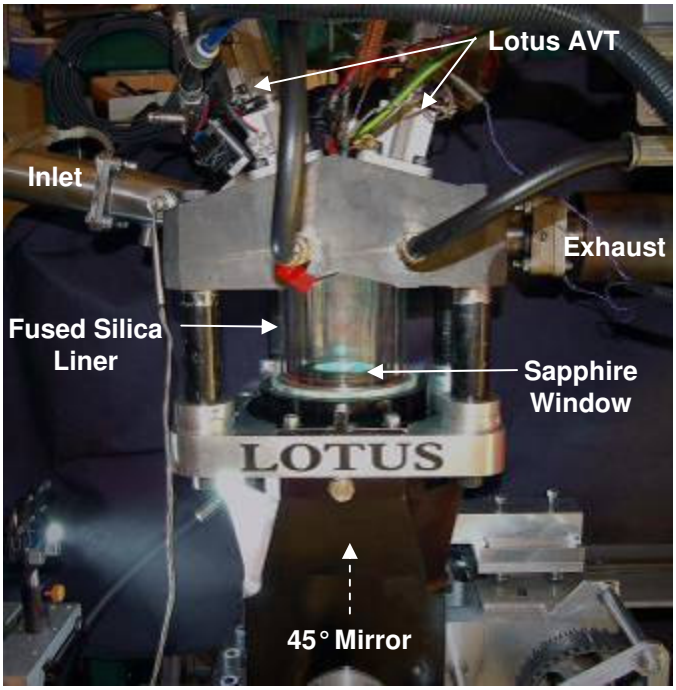

Figure 3: SCORE Optical Engine

The four overhead poppet valves (Figure 5) are actuated by means of a fully variable electro-hydraulic valve system, the AVT, which allows complete control of the individual valve profiles. The engine and valve profile specifications for this work have been provided in Figure 1. Linear displacement transducers are mounted to the top of each valve allowing the real-time position of the valve to be monitored and adjusted with a series of control gains until the valve profile matched the demanded profile accurately. Valve timing is given relative to TDC compression.

The engine contained a centrally mounted multistream gasoline fuel injector from Siemens VDO Automotive. The injector was fed 95 RON gasoline at 120 bar line pressure by a three cylinder gasoline fuel pump. This, in turn, was fed by a standard automotive fuel pump operating at 3.5 bar pressure. The injector was mounted into the cylinder at an angle of 10° inclined towards the spark plug. The injector contained six equally spaced orifices at an angle of approximately 45° from the injector axis (Figure 4).

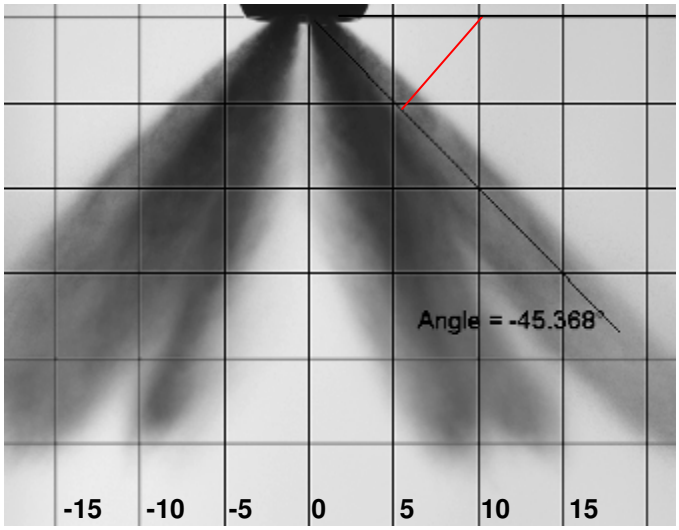

Figure 4: 6 hole multistream fuel injection spray into atmosphere: 120bar injection pressure, 1.75ms After SOES, 5 mm grid

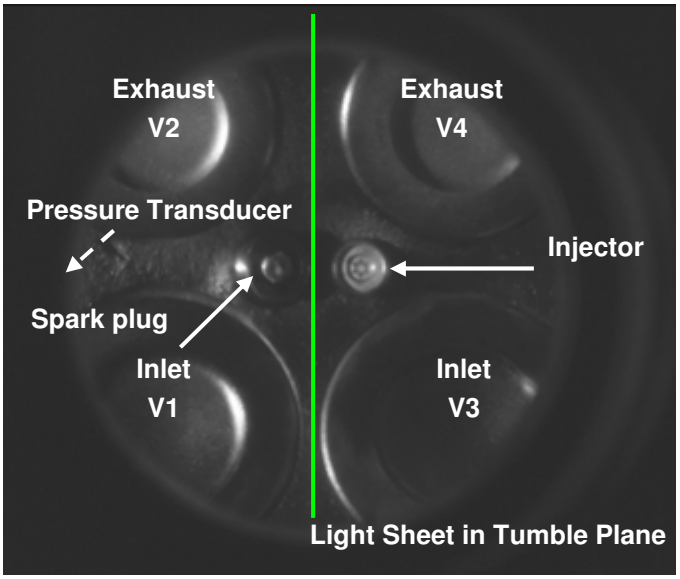

Figure 5: SCORE Combustion chamber

The injector driver incorporated a 1.0ms pre-charge time to facilitate fast opening of the needle solenoid. At 2000 rpm, this represented a 12° difference between the start of electronic signal and the start of needle lift. A further 2° was required before fuel left the orifice. As such there was a 14° offset between the start of electronic signal (SOES) and the start of fuel injection (SOI).

The electronic control signals to the injector driver were generated by an AVL 4210 engine timing unit which was referenced to the optical encoder on the crankshaft and the 2:1 drive.

The LaVision PIV system was based on the Flowmaster 3 fast shutter CCD camera and a New Wave “Solo 120” mJ/pulse Nd:YAG double pulsed laser. The laser beam was expanded by means of a -20 mm focal length cylindrical lens to form a light sheet of approximately 1 mm thickness and a width sufficient to fill the 55 mm aperture of the window. For the tumble plane measurements, this light sheet was directed off a 45° mirror, which had been mounted between the struts of the bifurcated piston, and up into the cylinder through the sapphire window. The light sheet was formed on the symmetrical plane between the two inlet valves (Figure 5).

For the swirl plane measurements, the laser beam was directed through the curved cylinder liner at a height 40 mm above the position of the piston at BDC, i.e. nominally half stroke. The Flowmaster 3 camera, fitted with a 60 mm focal length Nikon macro lens and using an aperture stop of f4, was positioned approximately 300 mm from the plane of the light sheet. The inlet air was seeded by a mist of approximately 1 µm diameter olive oil droplets produced by a Scitek seeding unit supplied with approximately 1 bar air pressure. The seeding was introduced into the engine airflow through four equally spaced radial ports mounted into the intake runner.

For the Mie imaging studies of the liquid fuel spray, the camera was mounted to capture the full bore and stroke of the engine. Images were taken in 0.6° increments from 470.0°, when fuel was first seen to enter the cylinder, to 540.2°. Five images were taken at each crank angle position and a mean image calculated.

PIV vector fields were taken at 10.0° intervals from 424.8° to 594.8° ATDC compression, at which point the piston filled the imaged area. The PIV results covered an area of 42.0 mm by 33.6 mm (Figure 6).

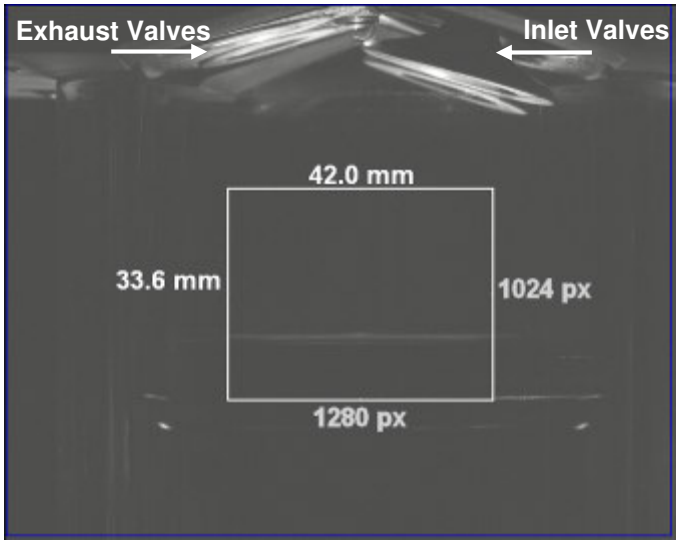

Figure 6: Imaged Area and PIV flow field region

All dimensions are given with respect to the centre of the piston crown when at BDC. Fifty image pairs were recorded. The PIV processing technique involved a subtraction of the background light level, followed by a multi-pass cross correlation technique on interrogation area sizes of 128px by 128px on the first pass and 64px by 64px on the second pass with 50% image overlap on both passes. Vectors were validated by application of the flow continuity principle and finally a mean flow field from the 50 image pairs was produced at each crank angle position. This produced vectors with approximately 1 mm resolution for the camera's field of view.

THERMODYNAMIC ENGINE

The single-cylinder thermodynamic engine (Figure 7) had a geometrically identical head geometry to the optical engine with the exception of detail differences in the piston crown required to locate the sapphire window. Poppet valve actuation was achieved by means of conventional belt driven camshafts acting directly upon "bucket" type tappets. Both intake and exhaust camshafts were installed in separate housings permitting each one to be readily exchanged. The camshaft drive belt pulleys were mounted in outrigger bearings allowing camshaft removal or replacement without disturbing the drive belt mechanism. The thermodynamic engine featured the same primary and secondary balance shaft assembly as the optical engine and was also capable of operation at 5000 rpm.

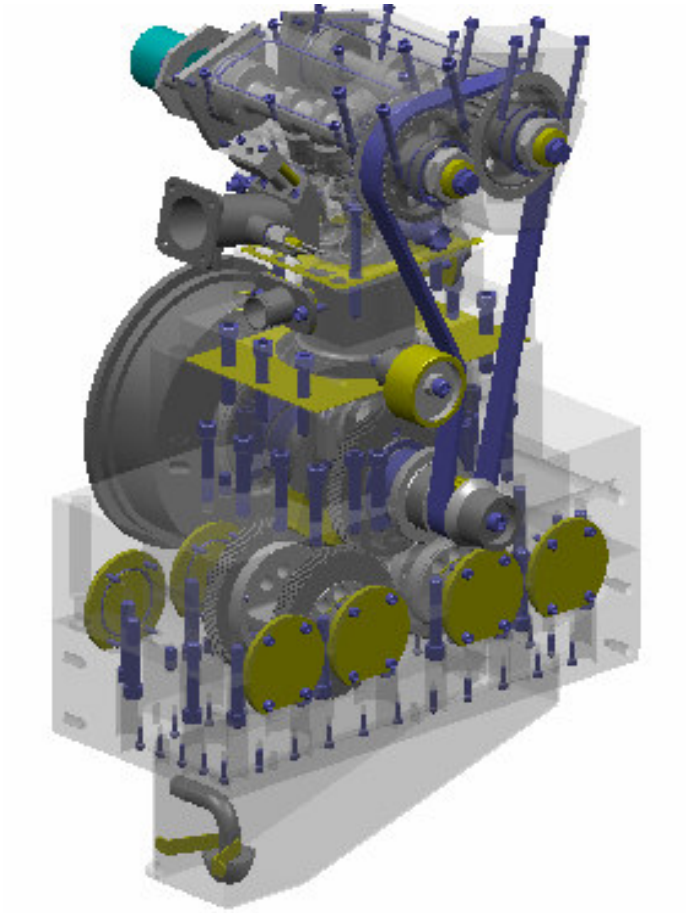
Figure 7: Ghosted view of thermodynamic engine with mechanical valve drive mechanism and outrigger bearing system

An AVL 4210 engine timing unit was again used to control injection and spark timing. The unit, as with the optical engine, took a reference signal from a camshaft mounted encoder with 0.2° resolution. The load on the engine was applied by a Borghi and Saveri water cooled eddy current dynamometer equipped with a load cell to measure torque.

Standard bench emissions were quantified using a Signal Instruments rack consisting of a heated vacuum chemiluminescent NOx analyser, a heated THC analyser (calibrated using CH_4), and an NDIR CO, and CO_2 multi gas analyser. Exhaust gas was sampled 250 mm downstream of the exhaust manifold in the exhaust plenum. A thermostatically controlled heated sample line was used to transmit the exhaust gas samples to the analysis equipment.

Fuel consumption, was measured by an AVL733 dynamic gravimetric fuel balance. The fuelling arrangement for the thermodynamic engine was the same as that for the optical engine apart from the plumbing to the fuel balance. Spilled flow from both the low and high pressure stages was cooled prior to return to the measuring vessel.

A Kistler 6041A piezo-capacitive pressure transducer was mounted between the intake and exhaust valves at the periphery of the combustion face of the cylinder head and used for measuring the in-cylinder pressure. The cylinder pressure was pegged at BDC of the intake stroke using a Kistler 4075A piezo-resistive transducer which was mounted towards the bottom of the cylinder liner. The pressure was pegged at BDC of the intake stroke. Intake manifold pressure was measured using a Druck 7517 absolute pressure transducer. Ambient pressure was recorded by means of a Prosser Digital barometer. Airflow measurements were made using a Siemens VDO hot-film meter and a Romet positive displacement gas flow meter. All temperatures were measured by means of K-type thermocouples connected to Nudam microprocessor units.

A fast data acquisition system from MTS Systems was used to acquire cylinder pressure and engine speed data. The system was clocked using the crank angle encoder at a resolution of 0.5°.

Initial experiments involved collecting data for port-fuelled, throttled operation. The engine was fired at 2000 rpm using the full valve lift intake camshaft (9.35 mm lift, 240° duration) and throttled to produce 2.7 bar $IMEP_{720°}$. The baseline performance was evaluated by means of a simple injection and spark timing sweep. At each spark and fuel timing, the throttle angle was adjusted to meet the required load point while the fuel injection pulse width adjusted manually to achieve a stoichiometric air fuel ratio (AFR). Three hundred engine cycles were recorded at each test condition and mean values calculated.

The engine was then fired in direct injection mode using the same full valve lift camshaft throttled down to the 2.7 bar $IMEP_{720°}$ load point. An injection and spark timing sweep was conducted to compare the effect of changing from port injection to direct injection. Fuel injection timing was varied from 390° ATDC compression to 540° ATDC (BDC intake). The combustion system used in this study was designed for homogeneous charge operation, consequently no emissions data was recorded for SOI timings beyond 540°. Four spark timings were investigated at 670°, 675°, 680° and 685°. Injection timing sweeps were conducted for the four inlet valve opening profiles discussed earlier (Figure 1). For the single valve profile, the tests were repeated on both inlet valves to investigate the effect of a change in direction of the bulk swirl motion. Under unthrottled conditions, the spark timing range was advanced by five degrees due to combustion stability degrading beyond a spark timing of 680°. Data are presented for MBT spark timing.

All data points have been recorded for both GDI injection and port fuelled operation to use as a comparative baseline. The ISFC of the engine under port fuelled operation compared to the fuel consumption using the four direct injection modes are presented in Figure 8.

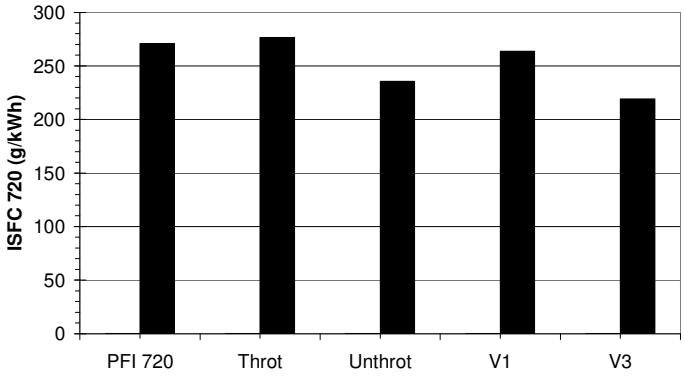

Figure 8: Net $ISFC_{(720°)}$ Variation at SOES 396°

RESULTS & DISCUSSION

The emissions of CO_2, CO, NOx, THC, and ISFC for injection timings between 376° to 526° in 10° intervals will be presented, along with PIV flow fields and Mie imaging data for injection timings of 470° under the three valve conditions. The emissions plots have been displayed with the valve lift profiles under investigation.

NET INDICATED SPECIFIC FUEL CONSUMPTION (NISFC)

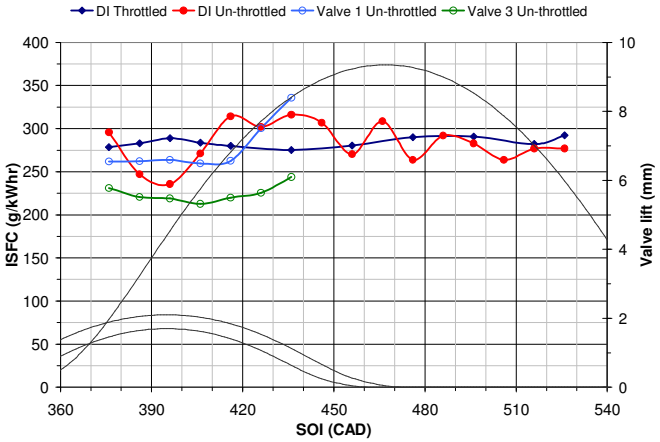

Figure 9: Net $ISFC_{(720°)}$ Variation against SOI

The net indicated fuel consumption plotted against start of injection for the three different valve profiles is presented in Figure 9. For throttled operation, the lowest $ISFC_{(720°)}$ was achieved with early injection timing with a minimum of 260 g/kWhr at SOI 386°. Retarding the injection timing caused a progressive rise in the ISFC. For the unthrottled case, with both valves operating, the ISFC fluctuated between a minimum of 235 g/kWhr at 396° and 316 g/kWhr at 436°. Following the peak at 436°, there is a gradual improvement in ISFC, however, fluctuations begin to appear as the SOI is retarded.

For two valve unthrottled operation, the $ISFC_{(360°)}$ suggests that the combustion performance is improved at an injection timing of 396°, however, as a result of increasing pumping losses involved with generating a depression within the cylinder, the $ISFC_{(720°)}$ shows no benefit beyond injection timings of 406°.

For single valve operation, the fuel injection timing sweep was not extended beyond 436° as the engine became extremely unstable with COV values greater than 30. It was believed that this was due to the reduced air flow across the injector nozzle orifice as the valve closed which reduced the local air-spray interaction and subsequent mixing before ignition.

Images taken from the optical engine for a SOI of 460° show that the fuel spray impacts on the open valve for throttled operation, but, for unthrottled operation, the short duration cam profiles are closed and the fuel spray enters the cylinder unimpeded (Figure 10).

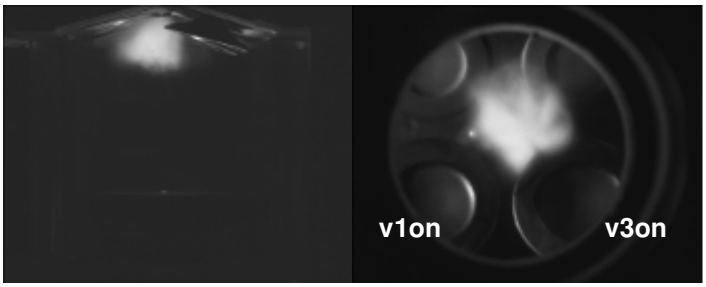

a) 2000rpm, 2.7bar $IMEP_{720°}$ (Throttled)

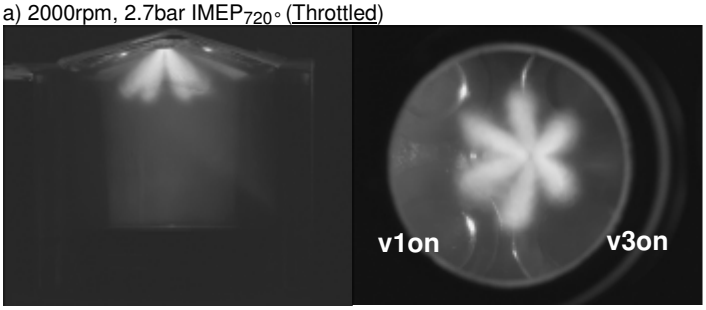

c) 2000rpm, 2.7bar IMEP720° (Unthrottled, 2 Valves)

Figure 10: 474.8° ATDC Compression, 0.4ms ASOI, Throttled v Unthrottled

The ISFC when Valve 3 only was operated was lower than when Valve 1 was operated. This may be caused by either, different flow coefficients through the two inlet ports or, a consequence of the complex interactions between the airflow structures and off centre fuel injector axis. Mie images and the corresponding airflow structures as quantified by the PIV analysis, are shown in Figure 11. The PIV vector fields show that when both valves are on, the tumble motion dominates and only weak structures can be seen in the swirl plane. These show the flow moving from the exhaust side of the cylinder to the inlet side. The swirl motion induced by opening one valve is not centred around the cylinder axis, but in fact is centred below the two exhaust valves at coordinates (-5, 10) mm. In this plane, which is located 40 mm above the piston at BDC, the bulk of the flow travels towards Valve 1 when Valve 1 is opened and towards Valve 3 when Valve 3 is opened. The Mie images in Figure 11 show that the fuel plumes are convected away from the open valve by the momentum of the air moving across the nozzle orifice.

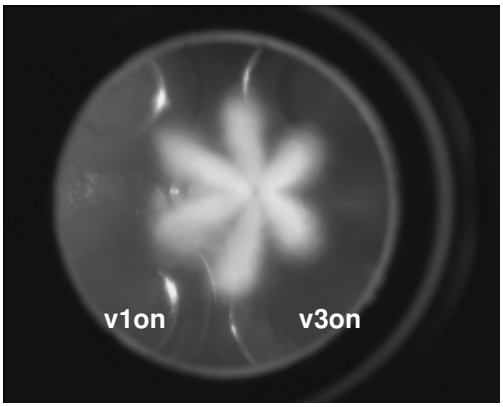

a) Unthrottled, Both Valves on

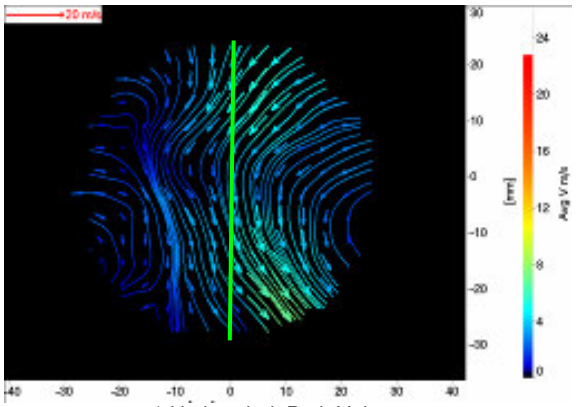

a) Unthrottled, Both Valves on

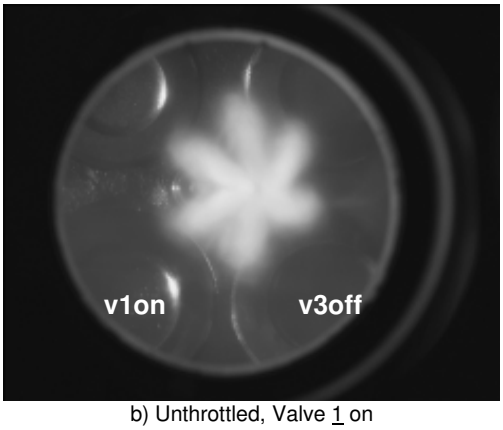

b) Unthrottled, Valve 1 on

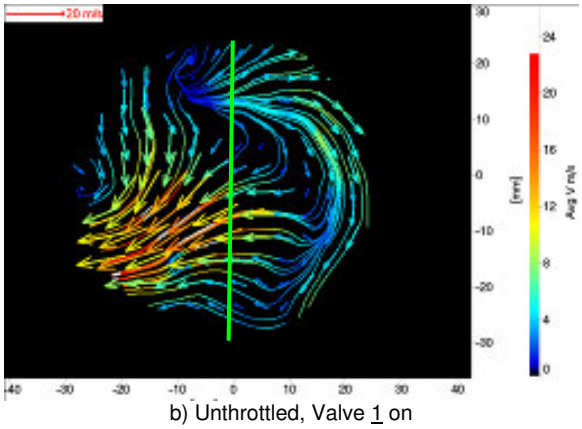

b) Unthrottled, Valve 1 on

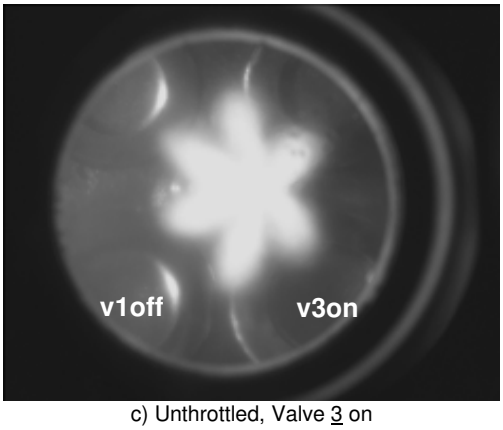

c) Unthrottled, Valve 3 on

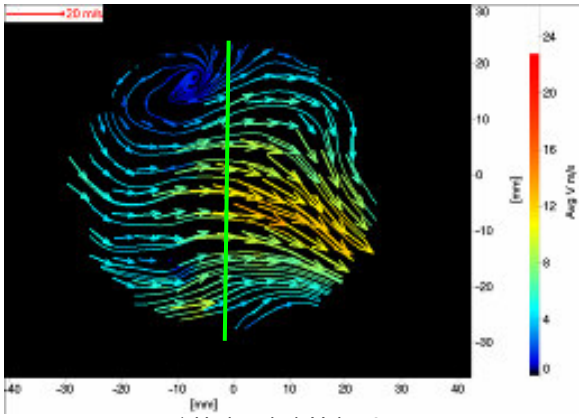

c) Unthrottled, Valve 3 on

Figure 11: 474.8° ATDC Compression, 0.4ms ASOI

CARBON DIOXIDE (CO_2)

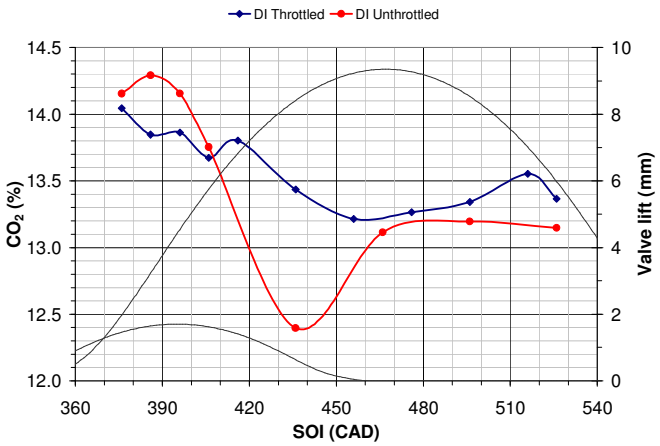

Figure 12: CO2 variation with SOI

The normalised emissions of CO_2 under throttled and un-throttled operation are shown in Figure 12. Production of CO_2 is a minimum for SOI's between 450° and 480°. This corresponds to the maximum lift of the valve. In this region, poor mixture preparation occurs which results in a lower proportion of fuel being oxidised to CO_2. The emissions of CO increases, and emissions of THC decrease during this period, implying a poor combustion regime occurring for these injection timings.

CARBON MONOXIDE (CO)

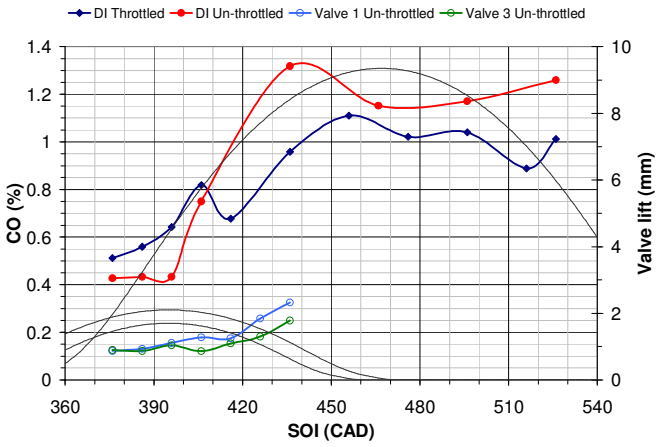

Figure 13: CO variation with SOI

The variation of CO with injection timing (Figure 13) shows the expected inverse trends to those for CO_2 emissions. CO was minimised for early injection timings for all valve conditions and increased as injection timing was retarded. The PIV flow field measurements offer an explanation for this trend. Early injection occurs into a high velocity flow field during the early period of the intake stroke (Figure 14), while later injections occur into much lower air flow velocities (Figure 15). This flow is directed across the injector tip and significantly disrupts the fuel spray from the injector. The high shear forces into which the spray is injected improve the air and fuel mixing and a more homogeneous mixture is formed. As fewer locally rich areas are present in the mixture at the time of spark, emissions of CO are reduced. In the unthrottled cases, the reduced opening area of the intake valves increases the air velocity even further, hence the unthrottled CO levels are slightly lower than the throttled case.

During induction the air-fuel charge may separate into lean and rich regions. The presence of rich pockets of air-fuel mixture will contribute more to the emissions of CO than the reductions created by the lean pockets. With increasing charge in-homogeneity, CO emissions will increase. As timing is retarded, less fuel will impact on the piston. Therefore, the majority of the air-fuel charge will burn slightly richer in comparison to that from earlier injection timings.

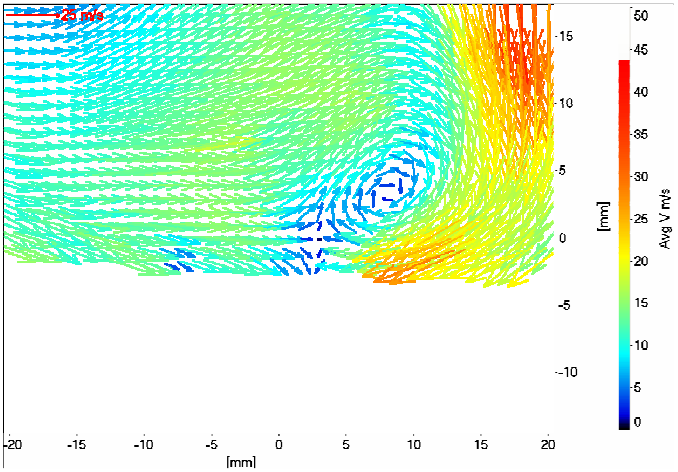

Figure 14: PIV flow field at 444.8° Unthrottled operation

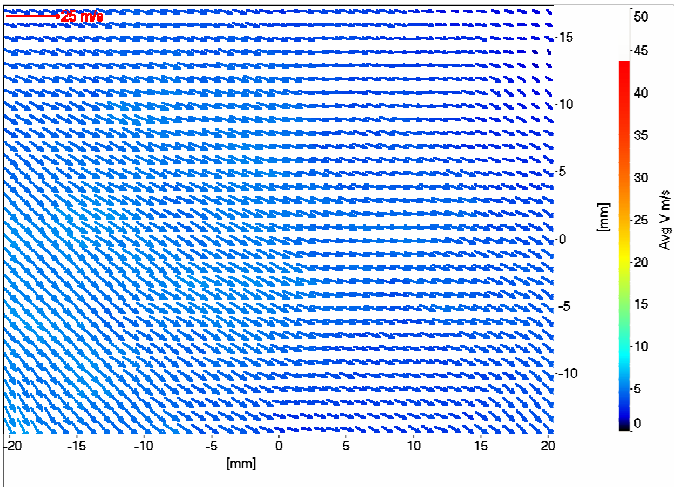

Figure 15: PIV flow field at 494.8° Unthrottled operation

NITROGEN OXIDES (NOX)

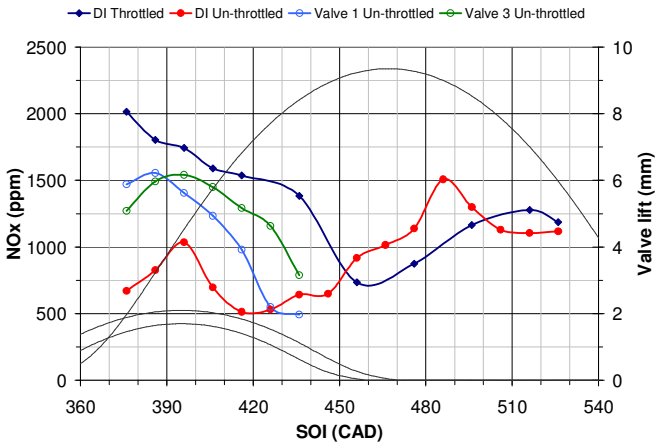

Figure 16: NOx variation with SOI

The production of NOx as a function of injection timing is shown in Figure 16. The NOx emissions under throttled operation show a gradual reduction for early injection timings until 420°, following which they begin to fall rapidly. NOx emissions were at a minimum between SOI 460° and SOI 480°, but retarding injection beyond 480° caused emissions to rise again.

NOx emissions were significantly reduced when the engine was switched to unthrottled operation and early injection timing was used. Retarding the injection timing beyond 426° caused NOx emissions to increase with a peak at 496° at which point emissions were comparable with throttled levels. However, a further retardation caused NOx levels to decrease again.

For early injection timings, the charge cooling effect was less substantial due to fuel impact on the piston crown. As such, the majority of the heat for vaporisation was drawn from the piston and not the ambient air. The lowest NOx emissions under unthrottled operation occurred between injection timings of 420° and 450°. During this region, the lean flammability limit of the mixture is probably reached due to poor mixture homogeneity. The poor combustion in this region leads to lower in-cylinder pressures and temperatures. The measured COV of the engine was highest during this region indicating poor combustion performance.

When single valve operation was employed, the NOx emissions increased slightly over twin valve operation but similar trends were exhibited with levels reaching a minimum at 440°. Slight changes were seen between intake valve 1 and 3 due to different mixing interactions between the symmetrical valve locations with the non-central positioning of the fuel injector. However, at these injection timings, the engine was extremely unstable and the reduction in NOx emissions were, more than likely, due to an increase in the number of misfires, supporting the suggestion of poor mixture preparation.

NOx emissions were found to be lower for DI operation than port fuelled running as the “charge cooling” effect, caused by drawing the latent heat for vaporisation from the air within the cylinder lowered the initial gas temperature and hence reduced the peak in-cylinder pressures.

TOTAL HYDROCARBONS (THC)

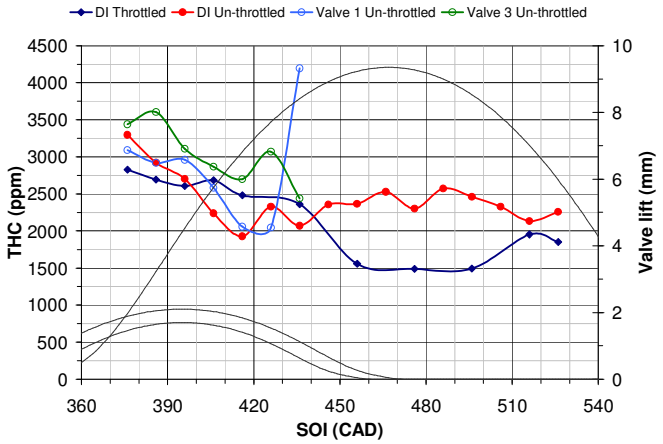

Figure 17: THC variation with SOI

The emissions of THC are shown in Figure 17. THC emissions were seen to reduce as injection timing was retarded from 370° to 450° for all the valve strategies. The main mechanism for THC production was impact of the direct injected fuel spray on the descending piston crown. This impact formed a locally rich fuel film which was the source of the THC emissions. As the injection timing was retarded, the piston was further from the injector orifice at the start of injection and consequently less fuel was deposited on the piston surface (Figure 18).

Beyond 450°, the level of THC remained relatively constant, as the piston was near BDC at the start of injection and began collecting fuel droplets on the start of the compression stroke. The level of THC was slightly higher for the un-throttled valve profiles as the reduction in in-cylinder pressure during the latter part of the intake stroke increased the penetration of the fuel spray and allowed more droplets to impact the piston (Figure 19).

For the single valve operation, a significant peak could be seen at injection timings beyond 426°. This confirmed that a high proportion of misfires were occurring and the engine was seen to be extremely unstable.

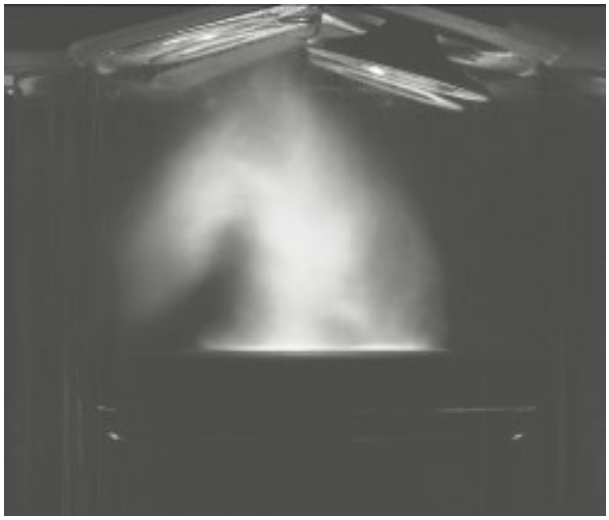

SOI at 450°, Image at 1.3ms ASOI 458°)

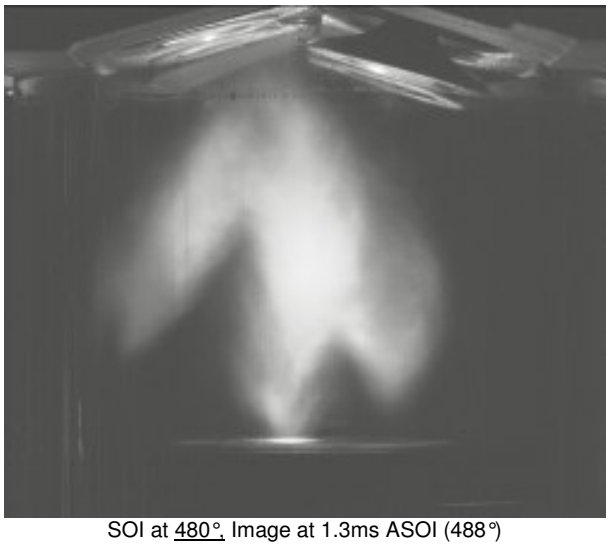

SOI at 480°, Image at 1.3ms ASOI (488°)

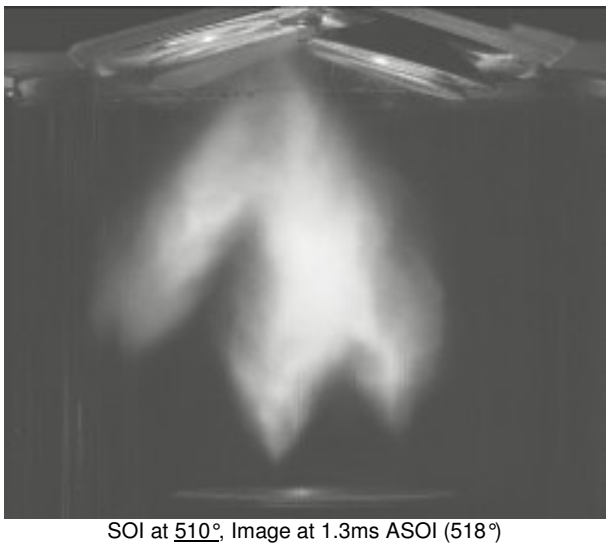

SOI at 510°, Image at 1.3ms ASOI (518°)

Figure 18: Fuel spray at 1.3ms ASOI (WOT, Standard Valve Timing)

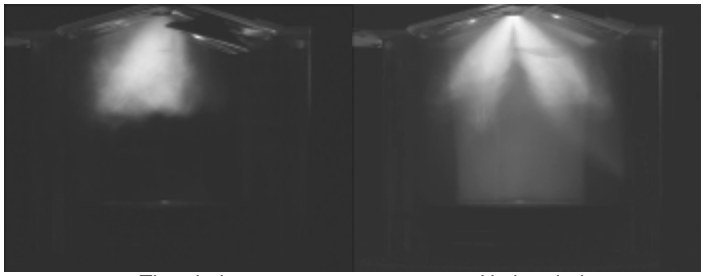

Throttled Unthrottled

Figure 19: Fuel injection spray at 122.6° (0.88ms ASOI)

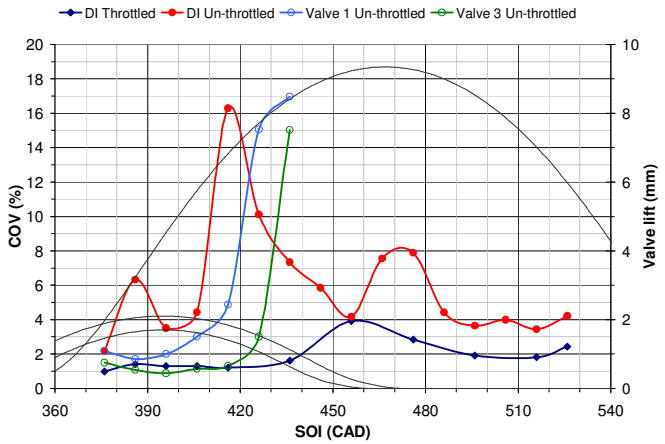

Figure 20: COV variation with SOI

Regarding the trends in the emissions, it can be seen that the drop off between 430° and 530° corresponds to an increase in CO and ISFC. It is thought that combustion is slow during this region leading to lower peak cylinder pressures and temperatures and hence NOx. The decrease in THC is accompanied by an increase in CO and decrease in CO_2. The increase in exhaust temperatures seen for these injection timings suggests a retarded combustion phasing which continues to oxidise HC during the expansion stroke. At this point, the temperature is believed to be insufficient to oxidise the CO into CO_2. Combustion in this region is also unstable as shown by the rise in COV (Figure 20).

PIV FLOW FIELDS

The mean PIV flow fields were used to assist in understanding the changes in airflow occurring in the cylinder under the different valve opening profiles. Figure 21 shows the mean PIV vector fields from the tumble plane at 474.8° for the three unthrottled valve strategies (Swirl plane flow fields have already been presented in Figure 11).

The PIV vector fields were used to calculate tumble and swirl ratios for the flow about the centre of the cylinder for the field of view of the camera. As only a region of the cylinder is captured, these ratios are not representative of the overall tumble and swirl ratio of the cylinder. The ratios assume conservation of angular momentum (Equation 1 & 2) [11].

$$TR = \frac{8\sum_{n=1}^{N}(V(i)_n.X(i)_n - U(i)_n.Y(i)_n)}{NwB^2} \quad (1)$$

$$SR = \frac{8\sum_{n=1}^{N}(W(i)_n.X(i)_n - U(i)_n.Z(i)_n)}{NwB^2} \quad (2)$$

A plot of tumble ratio against crank angle has been produced from selected vector fields (Figure 22). Vector fields were rejected for those crank angles when the piston was in the region of interest and, for the unthrottled cases (Early Inlet Valve Closing) where the reducing cylinder pressure caused condensation of in-cylinder water vapour to occur. When condensation did occur, the laser light was scattered by the fog of water droplets and saturation of the CCD chip occurred.

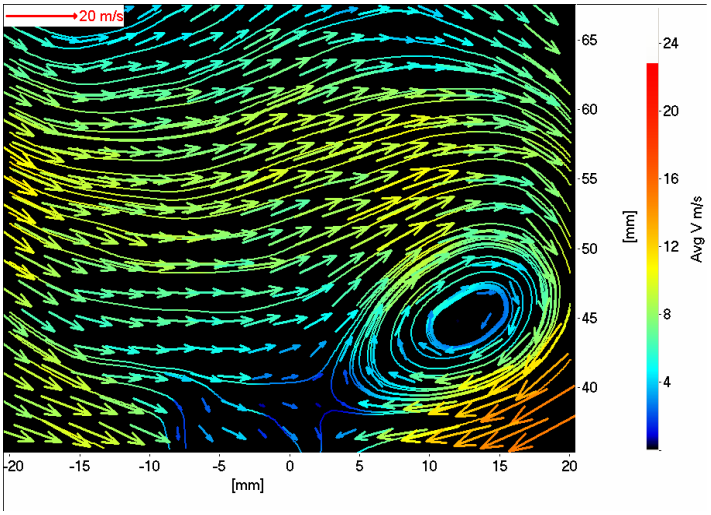

Unthrottled flow field (Both valves on) at 474.8° CA

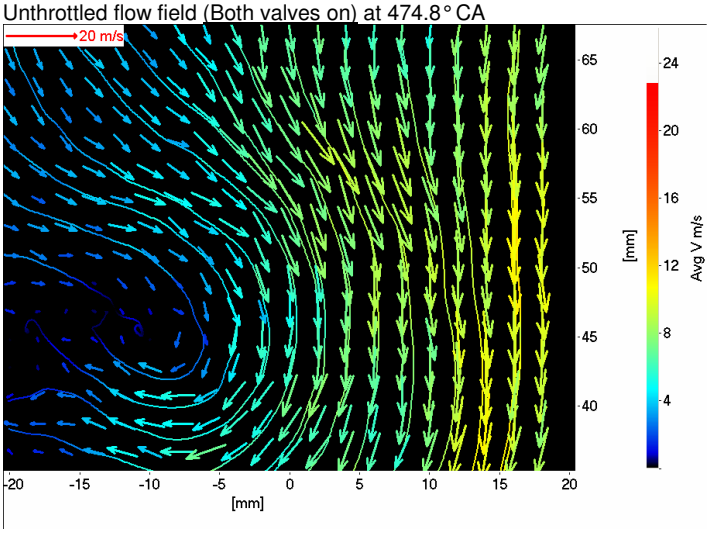

Unthrottled flow field (Valve 1 on) at 474.8° CA

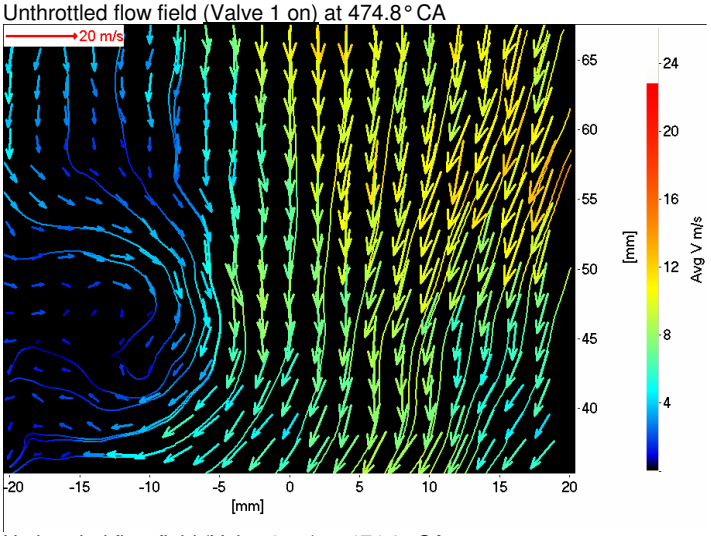

Unthrottled flow field (Valve 3 on) at 474.8° CA

Figure 21: Mean PIV flow field under unthrottled conditions

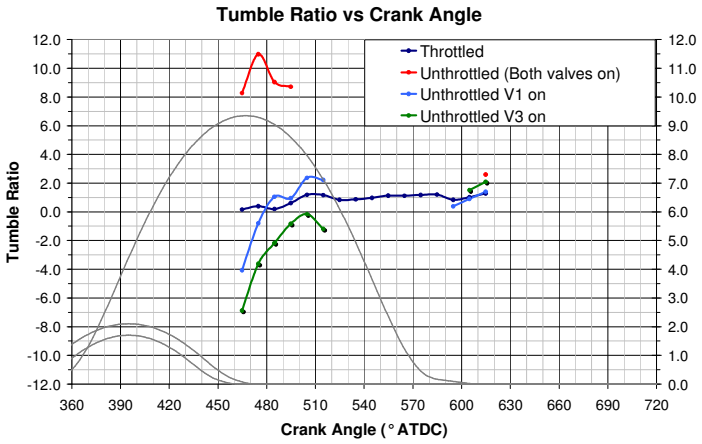

Figure 22: Tumble ratio against crank angle

The plot of tumble ratio against crank angle (Figure 22) shows that the tumble ratio is the strongest in the case of the unthrottled valve lift with both valves operating. It is believed that this is caused by the very low lift of the valve as it nears the end of its early intake valve closing profile combined with a higher manifold pressure. With the piston travelling at close to its maximum speed and hence the greatest rate of change of volume, the intake air is forced to accelerate as it passes through the narrow valve gap. This momentum forces the flow down the intake side of the cylinder, and when it meets the piston crown it is forced to turn, forming the strong tumble effect seen. When the single valve profiles are operating, the swirl component is much more significant, and the recirculation in the tumble plane moves from the bottom right of the image to the bottom left, which reduced the calculated tumble ratio.

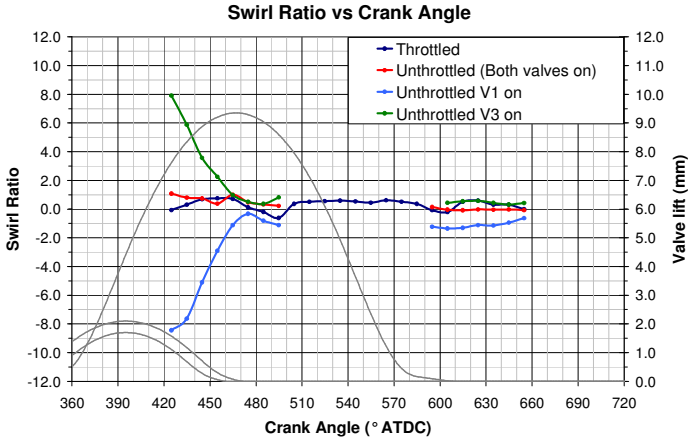

Figure 23: Swirl ratio against crank angle

Figure 23 shows a similar plot for the flow in the swirl plane. When both valves are operating, in either the throttled or unthrottled cases, two counter rotating vortices are formed. The right hand vortex dominates slightly, probably due to differences in the flow coefficients in the intake port and hence the swirl ratio is of the order of 0 to 2. When only one of the intake valves is operated, the swirl ratio shows that strong swirl structures are formed within the cylinder. Opening Valve 1 only produces a clockwise rotation and opening Valve 3 only produces an anticlockwise rotation of similar magnitude. The swirl ratio decays rapidly as the inlet valve closes and the piston descends and by 120° ATDC the swirl structures are only slightly stronger than those found when both valves are operated. Beyond 130°, condensation in the cylinder means PIV data can not be taken for the unthrottled cases, however, between 230° and 290° the swirl ratio for the single valve is again only slightly above the twin valve operation.

CONCLUSIONS

Operating an engine with variable valve actuation has significant potential for increasing engine efficiency and minimising emissions. This work investigated the variations in air motion and air-fuel mixing with valve timing strategies in the cylinder of an optical engine. The observed physical processes were related to engine performance, emissions output and fuel economy as measured on a thermodynamic engine with an identical combustion chamber geometry. The valve timing strategy adopted was un-throttled EIVC with a reduced lift to control engine load. Three operational variations were examined, both inlet valves opening followed by each single valve opening in turn. The data obtained were compared with those for the standard valve opening profiles under throttled conditions. All the data were for the standard engine load case of 2000 rpm and 2.7 bar $IMEP_{720°}$

A significant reduction in ISFC is exhibited when either both valves or valve 3 only are operated under unthrottled operation. The ISFC when operating valve 3 is markedly improved over valve 1, signifying that the air flow magnitude and direction across the nozzle orifice at the start of injection is critical to the air fuel mixture preparation occurring within the cylinder.

The timing of the SOI in relation to the valve closure point also plays an important role in determining engine performance. SOIs between 450° and 480° produced notably poor performance for all the unthrottled EIVC cycle profiles under consideration due to the sudden change in the air flow structures across the nozzle tip as the short duration cam profiles closed. In these regions, the fuel consumption benefit was markedly reduced, as poor mixing caused a greater proportion of the liquid fuel to be stored on the cylinder walls and burn late during the expansion stroke. Although the single valve profiles were capable of generating a strong swirl motion whilst open,

this swirl ratio within the cylinder decayed rapidly once the valve had shut.

Injection timing is also the crucial factor in determining fuel impact on the piston, which is the major production mechanism for HC emissions. Single valve operation requires a much earlier start of injection to facilitate stable engine combustion. Without significantly earlier injection timings, single valve engine operation is extremely unstable.

ACKNOWLEDGMENTS

This work was made possible by Lotus Engineering and Siemens VDO Automotive supplying the engines and fuel injection equipment and expertise and the support of the EPSRC via grants GR/S91734/01 and GR/S91727/01.

REFERENCES

1. Turner, J.W.G., Pitcher, G., Burke, P., Garner, C. P., Wigley, G., Stansfield, P., Nuglisch, H., Ladommatos, N., Patel, R., Williams, P., (2006), The HOTFIRE Homogeneous GDI and Fully Variable Valve Train Project – An Initial Report, SAE 2006-01-1260.
2. Gunston, B, "World Encyclopaedia of Aero Engines". Patrick Stephens Limited, Sparkford, Yeoville, Somerset, BA22 7JJ, UK, 1995, 3rd Edition, pp. 49-50. ISBN 1-85260-509-X.
3. Ashley, C, "The Mitsubishi Gasoline Direct Injection engine (GDI). Automotive Engineer. Vol. 21, no. 5, pp. 20-3. Oct.-Nov. 1996
4. Zhao, F., Harrington, D. and Lai, M.-C., "Automotive Gasoline Direct-Injection Engines". Society of Automotive Engines, Inc., Warrendale, PA, 2002. ISBN 0-7680-0882-4.
5. Final Report on the Government Working Group on Sulphur in Gasoline and Diesel Fuel Setting a Level for Sulphur in Gasoline and Diesel Fuel (1998), Canadian Environmental Agency Report
6. Tuttle, J., "Controlling Engine Load by Means of Late Intake-Valve Closing". SAE paper number 800794, 1980.
7. Tuttle, J., "Controlling Engine Load by Means of Early Intake-Valve Closing". SAE paper number 820408, 1982.
8. Turner, J., Kenchington, S. and Stretch, D., "Production AVT development: Lotus and Eaton's electrohydraulic closed-loop fully variable valve train system". 25th Vienna Motor Symposium, 2004.
9. Wunderlich, K., Enderle, C., Keller, U., and Kaufmann, T., "The Electronic Valve Control as a Fuel Saving Future Technology of Contradiction in Terms Between Variability, Complexity, and Cost". Oral presentation: 24th Vienna Motor Symposium, April 2003.
10. Salber, W., Wolters, P., Esch, T., Geiger, J., Dilthey, J., " Synergies of Variable Valve Actuation and Direct Injection"
11. Pitcher, G., Wigley, G.., "LDA Analysis of the Tumble Flow Generated in a Motored 4 Valve Engine", Laser Anemometry - Advances and Applications, EALA, Limerick , Sep 2001.

CONTACT

Phil Stansfield
Department of Aeronautical and Automotive Engineering
Loughborough University
Leicestershire
LE11 3TU, UK
Tel: +44 (0) 1509 227246
Fax: +44 (0) 1509 227275
Email: p.a.stansfield@lboro.ac.uk
Ext: 7246

DEFINITIONS, ACRONYMS, ABBREVIATIONS

ACEA	Association de Constructeurs Européen d'Automobiles
AFR	Air fuel ratio
ASOI	After Start of Injection
ATDC	After Top Dead Centre
AVT	Active Valve Train
BDC	Bottom Dead Centre
BOM	Bill of Materials
CAD	Crank Angle Degrees
CCD	Charged Coupled Device
DISI	Direct Injection Spark Ignition
EIVC	Early Inlet Valve Closing
EVC	Exhaust Valve Closing
EVO	Exhaust Valve Opening
GDI	Gasoline Direct Injection
GHG	Greenhouse Gases
HCCI	Homogeneous Charge Compression Ignition
IMEP720	Indicated Mean Effective Pressure (over 720°)
IVC	Inlet Valve Closing
IVO	Inlet Valve Opening
LIVO	Late Inlet Valve Closing
MBT	Minimum ignition advance for Best Torque
MOP	Maximum Opening Point
NDIR	Non-Dispersive Infra-Red
ND:YAG	Neodymium Yttrium Aluminium Garnet
OSCAR	Thermodynamic research engine
PIV	Particle Image Velocimetry
SCORE	Single Cylinder Optical Research Engine
SOI	Start of injection
THC	Total Hydrocarbons